Research Square

Preprints are preliminary reports that have not undergone peer review.
They should not be considered conclusive, used to inform clinical practice,
or referenced by the media as validated information.

Simulation-guided design of an electricity-free, locally sourced heater for LAMP-based tuberculosis and malaria testing in sub- Saharan Africa

Aruomachi Kingsley Olumati
olumati.ak@achievers.edu.ng
Achievers University Owo
Omotayo Tolulope Motunrayo
Achievers University Owo
Benedict Olumhense Adoghe
Achievers University Owo
Ademola Samson Adekola
Achievers University Owo
Deborah Osi-Goyeyi Daramola
Bells University
Emmanuel Dominic Ephraim
Achievers University Owo
Oghenefejiro Omonigho Ederhi
State university of medical and applied Sciences

Research Article

Keywords: Loop-mediated isothermal amplification, electricity-free diagnostics, phase-change material, exothermic heater, finite-element simulation, tuberculosis, malaria, sub-Saharan Africa, point-of-care testing

Posted Date: November 26th, 2026

DOI: https://doi.org/10.21203/rs.3.rs-11730404/v1

License: This work is licensed under a Creative Commons Attribution 4.0 International License.
Read Full License

Additional Declarations: No competing interests reported.

Abstract

Background: The WHO recommends loop-mediated isothermal amplification (LAMP) for tuberculosis, and it is also the method used for malaria, but it still requires a stable heat source of 60–68°C. In sub-Saharan Africa 15% of health facilities are without electricity, while just 40% are supplied with electricity in a reliable manner. However, chemical heaters that incorporate an exothermic reaction and a phase change material (PCM) can eliminate that requirement, but existing designs have been based on imported magnesium–iron alloy and specialty paraffin, and they have been tuned through experimentation and they have been tested under limited ambient conditions. No research has forecasted the performance of such a heater as a diagnostic (as opposed to being a thermostat) throughout the climates of the area.

Methods:
An open-source, axisymmetric finite-element model (scikit-fem) of a cup-type heater that integrates fuel reaction kinetics, steam venting, enthalpy-method PCM and conductive filler, as well as heat loss to the environment was developed. A semi-mechanistic LAMP model, incorporating temperature-dependent amplification and Bst polymerase inactivation, and stochastic template initiation, is used to simulate the sample temperature and the resulting time-to-positive and 95% limit of detection (LoD95) after a fixed read time of 60 minutes for each heater run. The solver was compared with the analytical Stefan solution and checked for mesh, time-step and energy convergence. Quicklime (CaO) was compared to Mg–Fe alloy; palm derived palmitic acid and raw beeswax were compared with commercial 64 °C paraffin. We then investigated the mapping of the dose and climate windows (5–45 °C, still air to wind), explored the possibility of insulating, water metering, and conductive filler, and estimated the reliability by Monte Carlo simulation in four representative climate zones of Africa, followed by a Sobol global sensitivity analysis. The total number of coupled simulations run was over 7,000.

Results: The 12 g charge of quicklime was able to bring a 25-µL sample to 60 °C in 5.5 min and maintain that temperature for more than 1 h at 25 °C, compared with 10 min for an ideal 65 °C block. A 12 g charge of quicklime was able to raise a 25-µL sample to 60 °C in 5.5 min and hold it there for more than 1 h at 25 °C, compared to 10 min for an ideal 65 °C block. All designs would not have made it to 82-96 °C without the inclusion of PCM. Raw beeswax melted over a wide range and only passed 7 of 36 climate conditions, while palmitic acid passed 34 of 36, and imported paraffin passed 35 of 36. The energy density of quicklime was found to be low and hence dose errors of ±18% were quite tolerable over the full 5-45 °C range, compared to ±4% for Mg-Fe. In colder environments, thicker insulation was beneficial, but in hot environments, it was not. For realistic material and manufacturing variability, the fixed quicklime design yielded valid results in 90.8% (95% CI 88.3–92.9%) of the simulated tests and a climate-indexed fuel sachet increased this to 94.2% (95% CI 92.0–95.8%). Ambient temperature was the most sensitive parameter in the global sensitivity analysis, followed by the fuel dose and fuel purity.

Conclusions: In simulation, a sub-Saharan Africa-produced heater can achieve LAMP performance similar to a laboratory heat block in its various climates without electricity. The model provides specific

design principles and a free tool that is reproducible to modify the heater for other assays. The next step is bench validation by thermocouple logging and LAMP testing.

Background

The diseases that molecular point-of-care (POC) tests are designed to tackle are most prevalent in Sub-Saharan Africa. In 2024, the Africa Region was estimated to experience 282 million cases of malaria and 610,000 malaria deaths globally [1] and notified 1.9 million TB cases in 2023 [2]. Nucleic acid amplification is more sensitive than smear microscopy or antigen tests and since 2016, WHO has advised using TB-LAMP to replace sputum microscopy [3]. Loop mediated isothermal amplification (LAMP) only requires a single temperature (usually 60–65 °C), and can be detected visually using colour-changing dyes [4,5,6]. The final hurdle is the power. Fully 15% of health-care facilities in sub-Saharan Africa do not have any electricity at all, and only about 40% have a reliable supply [7]. However simple a LAMP heat block is, therefore, cannot be taken for granted in the clinics where most patients first come. This is solved by electricity-free heaters. The non-instrumented nucleic acid amplification (NINA) platform developed by PATH used a calcium oxide/magnesium–iron exothermic reaction and an engineered phase-change material (PCM) for maintaining LAMP tubes at near 63 °C [8,9]. Liu et al. developed a self-heating microfluidic fuel cartridge of Mg–Fe fuel and a paraffin with a temperature of 65 °C and a chamber temperature of 64 ± 3 °C at 40 °C ambient temperature with PCM, compared to 75 °C without PCM [10]. Curtis et al. and Singleton et al. found HIV-1 with similar heaters that contained a solid–liquid PCM [11,12] and Shah et al. substituted the solid–liquid PCM with boiling methanol in a compact Mg–Fe heater [13]. Computational approaches to thermal management and heat-transfer optimisation have been investigated in other engineering applications, including high-power electronic systems and industrial heat exchangers [14]. However, the integration of exothermic fuel kinetics, phase-change thermal regulation and diagnostic amplification performance presents a distinct modelling challenge for electricity-free molecular testing. These feasibility studies had four gaps. First, all the designs were optimized experimentally. We are not aware of any physics-based model published that connects fuel chemistry, phase change and heat loss to the sample tube's internal temperature that can be transferred to other geometries or climates. Second, the performance of the heater is not reported in terms of the response to the test result, but instead is reported as temperature and hold time. A sample that reaches 61 °C or has just come into contact with 70 °C will amplify or lose sensitivity and only a coupled amplification model can determine which. Third, the ambient temperature ranges have been very limited, usually 20-40 °C or 22-45 °C [10,13]. African point-of-care conditions range from cold highland mornings (less than 10 °C) to the hot afternoons of the Sahel (over 40 °C) with wind at outdoor locations. Fourthly, the fuels and PCMs that are used (Mg–Fe ration-heater alloy, specialty paraffin) are imported and quicklime and palm-derived fatty acids and beeswax are manufactured on a scale in the area. Approximately 5,900t of beeswax was produced in 2024 in Ethiopia alone, which accounts for about a third of the African production [15]. This study will closes those gaps, with the help of simulation and the use of only free software. It does the following:

- An open finite-element model of an exothermic-reaction and PCM heater with a coupled LAMP model that transforms each temperature history to a time-to-positive and a limit of detection at a fixed read time (a heat-to-answer model);
- the first quantitative comparison between locally-sourced materials (quicklime, palm-derived palmitic acid, raw beeswax) and imported materials (Mg–Fe alloy, paraffin) used to date;
- climate-resolved reliability estimates for four representative sub-saharan climate zones under realistic manufacturing and material variability, ranked by Sobol global sensitivity analysis;
- Several counter-intuitive practical design rules: an insulation paradox, a steam loss trade-off in water metering, the dose tolerance advantage of low-energy-density fuel and climate-indexed fuel dosing.

Methods

Device concept and geometry

A re-usable foam cup (Fig. 1) is used as the modelled device. There is one use only fuel sachet at the bottom. On adding water, the fuel reacts and will heat an aluminium plate (1 mm). Above the plate is a bath of PCM (approx. 20 mm deep, 13–14 g), contained in a conductive filler (steel or aluminium wool). Each 0.2 mL polypropylene tube containing 25 µL of LAMP mix is inserted into the PCM with the bottom of the tube 6 mm above the plate. The top is closed with a 5 mm air gap and a 10 mm foam lid and the sides and base are surrounded by 10 mm of expanded polystyrene. The inner radius is 16 mm. The geometry was modeled as axisymmetric with the tube axis being the axis of symmetry and corresponding to a single central tube. Multi-tube would have the tubes mounted on a ring at the same elevation.

Heat transfer model

Transient conduction was solved in cylindrical coordinates (r, z) with the enthalpy method [16]:

$$\partial H/\partial t = (1/r)\,\partial/\partial r\,(k\,r\,\partial T/\partial r) + \partial/\partial z\,(k\,\partial T/\partial z) + q'''(t),$$

where H(T) is the volumetric enthalpy of each material, including latent heat, and q''' is the volumetric heat release in the fuel bed. The heat loss through the outer surfaces to ambient air is by a combination of convection and radiation with the coefficient h (convection/radia = 5–30 W m-2 K-1) being dependent on the ambient air stream (still indoor air to an outdoor breeze) and r = 0 being a symmetry axis. The model was solved using linear triangular finite elements, which were created with the use of scikit-fem [17] on a structured mesh aligned with all material interfaces. The implicit Euler method, using a lumped-mass enthalpy formulation, was employed for time integration with the nodal temperature change being iterated to a level below 10^{-3} K (10^{-4} K for reference runs) using the chord (Picard) method. The melting behaviour of each material, as reported in the literature (Table 1), was represented by a sum of Gaussian melting peaks to describe the melting behavior of the phase change material. The conductivity of the

liquid regions was multiplied by a factor of 1–4 (base value 2) and the metal-wool filler by a conductivity multiplier (base value 8, range 1–8) for natural convection in molten PCM. This is done by modeling the additional water added to the fuel bed with a latent heat of evaporation at 100°C which is irreversible after being evaporated, meaning that energy carried away by steam is lost, similar to what happens in a vented device. This also limits the temperature of the fuel bed around 100°C when water is present.

Fuel reaction model

Two fuels were compared. Quicklime hydration, $CaO + H_2O \rightarrow Ca(OH)_2$, releases 63.7 kJ per mole, or 1.14 MJ per kg of CaO [18]. The lattice enthalpy of Ca 2+ (aq) is about − 2000 kJ mol-1 and the lattice enthalpy of Mg 2+ (aq) is about − 2286 kJ mol-1 [20]. The product-layer diffusion model [20] was used to describe Conversion X: (1 − (1 − X)^(1/3))² = ∫k(T)dt with Arrhenius temperature dependence (activation energy of 30 kJ mol^{-1}) evaluated at the mean fuel-bed temperature. The time to 50% conversion at 25°C (t_{50}) was used to set the rate constant. This combines two parameters that are within the control of the designer: particle size and water delivery rate of a wick. The base t_{50} values were 12 min for CaO and 20 min for Mg–Fe. To allow for incomplete reaction and passivation, the fraction of reaction heat delivered to the bed was 0.9 for CaO and 0.7 for Mg–Fe and both were varied during the uncertainty analysis. The amount of water supplied was 0.75 g/g of CaO (stoichiometric demand is 0.32 g/g) and 4.5 g water for the case of Mg–Fe.

Phase-change materials

Four models of PCM were used (Table 1). Palmitic (hexadecanoic) acid is a saturated fatty acid derived from palm oil made in West Africa and Central Africa. It melts near 62–63°C with a latent heat of about 200 kJ kg^{-1} [21, 22]. Liu et al. [10] used the imported specialty technical paraffin with melting point 64°C. A broad melting range of raw yellow beeswax from approximately 30°C to 65°C was modelled from published DSC data [23] that displayed a prominent peak around 51°C and latent heat of 173 J g^{-1}. The latent heat was assumed to be zero and the sensible heat capacity of the paraffin was used in a no-PCM control.

LAMP amplification and detection model

A semi-mechanistic LAMP model was driven by the volume-averaged sample temperature T(t). The relative amplification rate was normalized to 1 at 65°C and was given by: ρ(T) = A(T)·η_low(T)·η_high(T). A(T) is an Arrhenius term (60 kJ mol-1), and between about 58°C and above, the strand-displacement and initiation efficiency will decrease at first-order rate with Bst polymerase activity f decay exhibiting half-life of 120 min at 65°C; the corresponding half-life at 70°C and 75°C are about 20 and 3 min, respectively, with an Arrhenius activation energy of 350 kJ mol − 1. It takes 2 effective minutes to initiate the growth of the amplicons, which then grow logistically at a rate of 1.24·ρ·f·min-1 to reach a plateau of 10^{11} copies, at which point colour or turbidity can be seen. The stochastic approach was used for low

copy detection. The probability of detection is 1 − exp(− N_0κG), where G is the effective amplification time available, and which is calibrated to LoD95 = 10 copies for an ideal 65°C block read at 60 min. κ was calibrated to this LoD95. They exhibited LAMP behaviour with an optimum temperature of 63–66°C, the amplification could be carried out between 60°C–68°C and times-to-positive were 15–25 min; and failed above 68°C (Fig. 2c,d). They are assumptions rather than fits to one assay, and their effect is discussed below.

Performance metrics

The worst case for warm-up is each simulation began with all parts at ambient temperature when water was added (t = 0), with the tube already in place. We measured the time to 60°C, the longest hold time between 60°C and 68°C, the maximum sample temperature, the percent of fuel heat lost as steam, the number of copies that took 10^3 seconds to start, and LoD95 at a 60-minute reading. Validity of a test was defined as: LoD95 ≤ 20 copies, with no more than a two-fold decrease in sensitivity compared to the perfect heat block, and a 10^3 copy sample becoming positive after 60 min.

Verification

The enthalpy solver was tested for the full device with three different meshes (495, 1,708, and 6,254 nodes) and time steps (2 s to 10 s) against the analytical solution of a two-phase Neumann problem [24] that was solved for planar melting of palmitic acid from an 80°C wall into solid at 40°C. In all of the runs, global energy conservation (stored enthalpy change against heat generated minus heat lost) was checked.

Parameter studies

Parameter studies covered: (i) fuel × PCM × ambient (2 × 4 × 3); (ii) a climate map of PCM × ambient temperature (5–45°C in 5 K steps) × h (5, 10, 20 and 30 W m^{-2} K^{-1}); (iii) fuel dose × ambient for both fuels; (iv) fuel dose × PCM height; (v) foam thickness (5–30 mm); (vi) fuel reaction speed (t_{50} 3–36 min); and (vii) filler conductivity (1–8×). The designs advanced were those that performed best under the coarse optimisation, based on the worst-case LoD95 at 5, 25 and 45°C, applied to the four factors: dose, PCM height, filler and t_{50}. We also re-created the operating conditions of two published heaters (Mg–Fe with 65°C paraffin at 20–40°C [10]; ambient 22 and 45°C [13]) as a qualitative trend check.

Monte Carlo reliability and global sensitivity

The ambience of a typical working day was split by four representative climate zones a point-of-care test might target: highland (e.g. Addis Ababa, Nairobi; 8–24°C), humid lowland (e.g. Lagos, Kinshasa; 23–33°C), hot semi-arid Sahel (e.g. Kano, Niamey; 25–45°C) and southern cool season (e.g. Johannesburg, Lusaka; 3–22°C). These ranges are representative and should be adjusted to accommodate local station

data. A total of 150 tests were simulated for each zone and design, with the ambient temperature uniformly distributed within the zone range and the fuel dose, water volume, fuel reaction speed, PCM melting point, latent heat, liquid convection factor, filler conductivity, and foam thickness randomly distributed within their respective ranges, and with h and the fuel activity determined for each test. Five designs have been compared: CaO 12 g with palmitic acid (fixed dose); CaO with a climate-indexed sachet (16 g below 15°C, 12 g at 15–32°C, 9 g above 32°C, chosen by a thermometer printed on the kit); CaO 12 g with paraffin; Mg–Fe 0.7 g with palmitic acid; and Mg–Fe with a climate-indexed sachet (0.8, 0.7 and 0.6 g). Each validity rate is provided with a Wilson 95% confidence interval. Saltelli sampling was used to conduct experiments using 11 inputs over the entire region (ambient 3–45°C) and the $\log_{10}$ LoD95 was computed, with 128 runs per input for each fuel, corresponding to a total N of 1,664 runs, in SALib [25–27] so that heavy-tailed failures didn't dominate the variance (which were capped at 30 copies).

Software and computation

All code was written in Python 3 with NumPy, SciPy, scikit-fem, SALib and Matplotlib, and runs on a laptop. It takes approximately 1–3 s to make a production run. The entire study was performed with over 7000 coupled runs. Additional file 1 contains the code, input files and scripts used for the regeneration of all the figures.

Table 1
Model parameters

Component	ρ (kg m⁻³) / c (J kg⁻¹ K⁻¹) / k (W m⁻¹ K⁻¹)	Phase change or reaction	Source
Expanded polystyrene	25 / 1300 / 0.035	—	Typical values
Aluminium plate	2700 / 900 / 200	—	Typical values
Polypropylene tube	900 / 1900 / 0.20	—	Typical values
LAMP mix (aqueous)	1000 / 4180 / 0.60	—	Water
Palmitic acid	900 / 2300 / 0.22	62.5 (σ 0.8 K); 200 kJ kg⁻¹	[21, 22]
Paraffin (64°C grade)	850 / 2200 / 0.21	64.0 (σ 1.2 K); 200 kJ kg⁻¹	[10]
Raw yellow beeswax	950 / 2300 / 0.25	Peaks 40, 51, 60°C (weights 0.2/0.5/0.3); 172 kJ kg⁻¹	[23]
CaO fuel	Bulk 1100; c 750	1.136 MJ kg⁻¹; t_{50} 12 min; E□ 30 kJ mol⁻¹	[18, 20]
Mg–Fe fuel (95% Mg)	Bulk 1000; c 1000	13.8 MJ kg⁻¹; t_{50} 20 min; E□ 30 kJ mol⁻¹	[19, 20]
LAMP kinetics	—	E□ 60 kJ mol⁻¹; T_low 58°C; T_high 69.5°C; Bst t½ 120 min at 65°C	Calibrated to [4–6]

Results

Verification

The enthalpy solver was able to generate the Neumann melting front within 1.1%, after 5 minutes (Fig. 2a). The difference between the true and the smoothed latent heat is represented by the residual error, which is a result of using 0.3 K melting width for smoothing the latent heat. When compared to the coarsest production setting (495 nodes, 10 s steps) and the reference (6,254 nodes, 2 s), the peak sample temperature varied by less than 0.1 K and the time to sample temperature of 60°C varied by less than 0.05 min on the full device (Fig. 2b). For parameter studies, the coarse setting was thus used, whereas for Fig. 3 the reference setting was chosen. The median difference in the energy-balance was 0.05 J, against approximately 12 kJ heat released. Twenty-three percent of the production runs (65 of 3,300) were below 1%, but none had any particularly slow fuel release, and no conclusions were changed if they were excluded.

Behaviour of the optimised quicklime heater

The optimised quicklime design with 12g CaO, 9g water, 8x filler (palmitic acid) is shown at 25°C in Fig. 3. Within a minute, the fuel bed temperature was increased to approximately 97°C and remained at this temperature for approximately 10 min, during which steam was released as excess water evaporated. The heat entered the plate and propagated the melt front around the PCM, which reached the tube after 5 min. The sample even reached the 60–68°C range for over 69 min (until the end of the run) while the PCM was not more than 70% melted. The results of the test showed that 10^3 copies gave a positive result at 21.8 min, with a LoD95 of 12.1 copies, which is reasonably similar to the ideal 65°C block value of 10 copies. The total heat released was 12.3 kJ of which 5.1 kJ (41%) was lost as steam and 3.8 kJ (31%) was lost through the walls over 75 min.

PCM choice decides whether the heater works

In all designs, latent heat was not present, resulting in all designs overheating (Fig. 4, Table 2). No test was valid, because no sample reached a temperature high enough to inactivate Bst polymerase even with quicklime, and the test with Mg–Fe inactivates Bst polymerase within minutes. Both palmitic acid and paraffin successfully locked the sample within the window at the ambient temperatures investigated, at 10°C, 25°C and 40°C, the latter having a higher melting point and thus a higher rise rate, but a peak at 40°C of 68.2°C, near the 68°C limit, while palmitic acid did not exceed 66.5°C. Raw beeswax could not be used both ways. In 36 conditions on the climate map (Fig. 5), palmitic acid was found to have absorbed 34, paraffin 35 and beeswax 7 of its latent heat before use and so the sample was stopped at 58.6°C, 52.6°C and 66.2°C respectively. Palmitic acid was not effective in any situation except strong wind at 5°C and paraffin was not effective in still air at 45°C.

Table 2
Fuel and PCM comparison (h = 10 W m⁻² K⁻¹)

Fuel	PCM	Ambient (°C)	Time to 60°C (min)	Time in 60–68°C (min)	Peak sample T (°C)	Time to positive, 10³ copies (min)	LoD95 (copies)	Heat lost as steam (%)	Valid
CaO 12 g	Palmitic acid	10	8.5	52	63.5	25.5	14.1	34	Yes
CaO 12 g	Palmitic acid	25	5.5	68	64.8	21.8	12.1	41	Yes
CaO 12 g	Palmitic acid	40	3.5	70	66.5	19.1	11.6	48	Yes
CaO 12 g	Paraffin	10	7.0	52	65.2	23.1	12.4	34	Yes
CaO 12 g	Paraffin	25	4.5	69	66.5	20.4	11.7	42	Yes
CaO 12 g	Paraffin	40	3.0	56	68.2	19.8	13.8	49	Yes
CaO 12 g	Beeswax	10	—	0	58.6	—	fail	32	No
CaO 12 g	Beeswax	25	14.5	30	62.3	31.2	29.0	39	No
CaO 12 g	Beeswax	40	7.0	32	72.8	50.1	fail	47	No
CaO 12 g	None	10	5.0	10	81.9	—	fail	36	No
CaO 12 g	None	25	3.0	13	87.5	—	fail	45	No
CaO 12 g	None	40	1.5	14	92.4	—	fail	55	No
Mg–Fe 0.7 g	Palmitic acid	10	7.5	55	63.7	24.6	13.7	7	Yes
Mg–Fe 0.7 g	Palmitic acid	25	5.0	68	65.8	20.9	12.1	14	Yes
Mg–Fe 0.7 g	Palmitic acid	40	3.0	60	68.3	19.8	13.0	21	Yes

Fuel	PCM	Ambient (°C)	Time to 60°C (min)	Time in 60–68°C (min)	Peak sample T (°C)	Time to positive, 10^3 copies (min)	LoD95 (copies)	Heat lost as steam (%)	Valid
Mg–Fe 0.7 g	Paraffin	10	6.5	56	65.7	22.4	12.3	8	Yes
Mg–Fe 0.7 g	Paraffin	25	4.5	69	67.8	20.5	12.6	15	Yes
Mg–Fe 0.7 g	Paraffin	40	2.5	54	70.2	25.4	22.0	22	No
Mg–Fe 0.7 g	Beeswax	10	—	0	57.2	—	fail	4	No
Mg–Fe 0.7 g	Beeswax	25	11.0	29	61.5	29.7	30.8	11	No
Mg–Fe 0.7 g	Beeswax	40	5.0	27	74.9	—	fail	17	No
Mg–Fe 0.7 g	None	10	4.5	8	89.3	—	fail	12	No
Mg–Fe 0.7 g	None	25	2.5	10	93.3	—	fail	25	No
Mg–Fe 0.7 g	None	40	1.5	16	95.7	—	fail	38	No

Low energy density makes quicklime forgiving

Figure 6 is a plot of validity vs. fuel dose and ambient temperature. All doses (11 g to 16 g) produced a valid test with quicklime at all ambient temperatures (5°C to 45°C), with a tolerance of at least ± 18% of the window's centre. Only in the cold did low doses fail, due to the slow rate of warming up of the sample. The range for Mg–Fe was very small, with only 0.65–0.70 g being valid, with a tolerance of

approximately ± 4%. The working range decreased by 10 to 15°C with a 0.1 g error (one seventh of the charge) due to either removal of the cold end or increase in the hot end. A small weighing error is a great heat error since Mg-Fe stores approximately 12 times more energy per gram than CaO. Quicklime also adds 12 g of solid and 9 g of water with a buffer heat capacity to release. If the sachet is filled by hand or with a simple volumetric scoop, it is more important than energy density

Design trade-offs: insulation, water metering and filler

There were three non-intuitive findings (Fig. 7). Firstly, to add more insulation is not always the best solution. The LoD95 increased from 21.4 copies at 10°C when foam was increased from 5 mm to 30 mm to 14.1 copies, while at 40°C it decreased from 14.8 copies to 23.2 copies, since a well-insulated cup will not be able to dissipate the excess heat from the fuel when the PCM is totally melted. Secondly, the time needed for water to reach the fuel is a compromise between waste and overheating. Slow release (t_{50} = 36 min) reduced steam losses to 20% while providing heat to a molten PCM at 40°C, which caused failure. The best t_{50} is 12–18 min meaning the wick can provide water for about 1/4 hour. Third, conductive filler is the only inexpensive improvement for the PCM. With the use of expanded graphite or metal wool as a heat spreading material, the warm-up time at 10°C was reduced to 9.5 min (from 20.0 min) and the hot-side failures have been eliminated by distributing the heat throughout the PCM before it is heated too much near the plate.

Consistency with published heaters

The model results peak sample temperature of 70.1°C when operating with Mg–Fe and paraffin at 40°C ambient and PCM, and 93.4°C ambient when operating without the PCM, which matches the results from Liu et al. [10]. Liu et al. measured 64 ± 3°C and 75°C. The model is capable of reproducing the main finding, namely the PCM is the one which keeps the sample in the LAMP window in hot conditions. With our thick fuel-thermal-mass container compared to their thin microfluidic container, it predicts a larger overshoot without PCM. Between 22°C and 45°C ambient, the model's time to reach 60°C fell from 9.0 to 4.0 min, the same direction as Shah et al. (7.1 to 5.7 min) [13]. They increased their hold time at 45 °c and ours decreased from 64 to 53 min. This is normal: Boiling-methanol regulator absorbs additional heat as long as liquid exists whereas PCM solid/liquid has a finite capacity. These are trend comparisons and not quantitative validations due to the different geometries.

Reliability across climate zones

For realistic variability (Fig. 8a, Table 3) the fixed quicklime and palmitic acid design had valid results in 90.8% (95% CI 88.3–92.9%) of the simulated tests across the four zones, while the fixed Mg–Fe design had valid results in 88.0% (95% CI 85.2–90.4%) of the simulated tests across the four zones. All designs were best suited to warm humid lowlands. The cool zones were the most difficult. There, there were only a few failures which were mostly marginal (LoD95 of 20–35 copies) and from the slow warm up and also a plateau just above 61°C, where cold, wind and partly slaked lime and low melting PCM batch coincided. The few failures in Sahel were due to over heating. A climate-indexed sachet in which the user selects one of three printed fuel sizes from a thermometer strip on the kit had a higher level of validity

(94.2% [95% CI 92.0–95.8%] for quicklime and 93.8% [95% CI 91.6–95.5%] for Mg–Fe). For cold zones, paraffin outperformed palmitic acid with an overall 92.2% (95% CI 89.7–94.1%), which is reflected by its 1.5 K higher melting point, and for the Sahel it did poorly with an overall 90.4% (95% CI 89.6–91.7%).

Table 3
Percentage of valid tests (95% CI) in Monte Carlo simulation, 150 tests per zone

Design	Highland	Humid lowland	Hot semi-arid Sahel	Southern cool season	All zones
CaO 12 g + palmitic acid	85 (79–90)	99 (96–100)	96 (92–98)	83 (76–88)	90.8 (88.3–92.9)
CaO climate-indexed + palmitic acid	91 (86–95)	98 (94–99)	97 (93–99)	90 (84–94)	94.2 (92.0–95.8)
CaO 12 g + paraffin	94 (89–97)	98 (94–99)	91 (85–94)	86 (80–91)	92.2 (89.7–94.1)
Mg–Fe 0.7 g + palmitic acid	83 (77–88)	100 (98–100)	93 (87–96)	76 (69–82)	88.0 (85.2–90.4)
Mg–Fe climate-indexed + palmitic acid	93 (87–96)	99 (95–100)	100 (98–100)	84 (77–89)	93.8 (91.6–95.5)

The Sobol analysis for the influence of inputs on the quicklime (when considering the full regional range, Fig. 8b, c) was ambient temperature (ST = 1.05), fuel dose (ST = 0.26), and fuel purity (ST = 0.19). The most important inputs for Mg–Fe were ambient temperature (ST = 0.67), fuel purity (ST = 0.36), and fuel dose (ST = 0.33). Fuel dose and fuel purity also had a greater importance for Mg–Fe (total-effect indices 0.33 and 0.36) than for quicklime (0.26 and 0.19). For the whole 3–45°C range the Mg–Fe design was valid in 73% of Sobol samples, compared to 84% for quick lime, consistent with the narrower dose range. The confidence intervals are large (Fig. 8) for N = 128, and so the ranking should be read rather than the values of the intervals. Total-effect indices, which are larger than the first order indices, indicate that failures occur when combinations of effects are present, such as cold weather, and underdosed or partly slaked fuel charge. Small index inputs, such as the filler conductivity, the thickness of the foam and the wind exposure for the ranges used in the tests for this input, can be had as a loose manufacturing tolerance. Within ± 1.5 K, the melting point of PCM was not significant, but the selection of two different melting points of PCM 1.5 K apart did cause the performance of cold zoning and hot zoning to be somewhat different (Table 3).

Cost and safety

The cost of the material required for each test is indicative and relatively low for both fuels, although it varies in type (Table 4). These order of magnitude costs are for illustrative purposes only and need to be

replaced by local quotes. Quicklime is sold throughout the region for construction and water treatment, and is relatively cheap (a US cent per test) but should be stored in waterproof containers as slaking in storage will lower its activity. The loss is reflected in the activity range of 0.70–0.95 in the Monte Carlo analysis. The Mg–Fe alloy imported is used and 0.6L of hydrogen is released for every 0.7g charge. This is safe in a ventilated room, but prevents air shipment [19]. Quicklime does not give off any gas, but it's caustic and the sachet should prevent this. Palmitic acid and paraffin are not used up. Only the fuel sachet, the wick and the tube are consumed per test and the remaining parts of the PCM, the filler and the cup are reused.

Table 4
Indicative consumable costs (assumptions; to be confirmed with local prices)

Item	Assumed price (US$)	Cost (US$)	Note
Quicklime (CaO), 12 g	0.10–0.50 per kg (construction grade)	0.001–0.006	Consumed
Mg–Fe alloy powder, 0.7 g	10–30 per kg (imported)	0.007–0.021	Consumed; H_2 by-product
Palmitic acid, ~ 14 g	1–3 per kg	0.013–0.04 per device	Reused; cycling stability to be confirmed
Paraffin 64°C grade, ~ 12 g	5–15 per kg (imported specialty)	0.06–0.18 per device	Reused

Discussion

This study demonstrates (simulation) that a heater fabricated from quicklime and palm derived palmitic acid is capable of operating LAMP in the sub-Saharan climates with a high degree of sensitivity compared to a lab heat block. The value of this work over previous experimental work is less in the device itself, which was based on the NINA concept [8, 9], than in 3 respects that previous work could not provide; a model that predicts diagnostic outcome other than temperature alone, a basis for using regional materials, and an estimate of the frequency of use in the field.

Heat-to-answer modelling.

The units of temperature (e.g., "63 ± 3°C for 40 min") have been provided as a proxy for the most important element, detection of a low-positive sample. The combination of the thermal model with stochastic model of initiation of LAMP revealed that the brief excursion to 68–69°C or the plateau at 61°C each incurs about a factor of two in LoD95, whereas the polymerase is destroyed by overshoot above 70°C for even a few minutes. This converts a thermal tolerance into a clinical one and enables the designers to exchange the warm-up time, hold time and peak temperature all in one unit.

Local materials.

Palmitic acid performed as well as imported paraffin, in 34 of 36 climate conditions. A drawback is that its melting point is a bit lower than that of other metals, but a benefit is that it is a bit higher than it is in hot environments. However, raw beeswax which is prolific in Ethiopia, Kenya and Tanzania is too poor for immediate use due to the fact that most of it melts well below the LAMP window [23]. It would be worthwhile to test a fractionated high melting point cut of beeswax or a mixture of palmitic and stearic acid adjusted to 63–64°C. The low energy density of quicklime is typically a disadvantage, but not when the quicklime is used in a hand-filled consumable. The width of its dose window was larger by a factor of 5 than that of Mg–Fe.

Design rules for implementers.

(1) Always use a PCM with a capacity for the hottest weather that is expected at the site. (2) Set the plateau with the PCM melting point. Palmitic acid is suitable for hot and temperate locations at 62–63°C, and at 64°C for cold locations. (3) Add conductive filler. (4) Do not over-insulate devices for hot climates. (5) Measure the water so that the fuel will react over a period of about 15 min. (6) For a wide range of climates, colour code two or three size of fuel sachets to a thermometer strip.

The observed sensitivity of heater performance to insulation thickness and heat-transfer characteristics highlights the importance of thermal design optimisation, a broader engineering consideration also addressed in studies of electronic thermal management and industrial heat-recovery systems [28].

Limitations. This is a simulation study and experimental verifications of the results demonstrated are required. The LAMP model is generic and the parameters are set to fit the typical behaviour, not fit a TB or malaria kit. According to Commercial TB-LAMP, the temperature is 67°C, and should be replaced with a kit-specific temperature–efficiency curve prior to any clinical claims. The fuel kinetics were approximated with a lumped parameter model of the diffusion type based on an assumed temperature dependence. In practice, release rate will vary with particle size, wick characteristics and the method the user uses for watering which must be calibrated. An effective conductivity, not resolved, was used to represent the natural convection in the molten PCM. The axisymmetric geometry is used to model a single tube in the middle. The climate-zone ranges are only indicative and humidity effects on stored quicklime were only represented by activity range. Costs are indicative.

Validation plan. A bench study should include: (i) recording fuel, PCM and tube temperatures at controlled ambient temperatures of 10, 25 and 40°C with and without a fan, and comparing these values with model predictions; (ii) performing a dilution series of a TB or malaria LAMP assay in the heater against a heat block in the heater to test the predicted LoD95 shifts; (iii) characterising the local lime grade by measuring quicklime release rates for the different wick sizes, and calibrating with the model the value of t_{50} and the value of activity; and (iv) measuring palmitic acid by DSC to characterize it. All of these measurements are input directly into the model due to the open code.

Conclusions

The results from a verified and open source heat-to-answer reaction model indicate that, with the use of two materials that are readily available in sub-Saharan Africa—quicklime and palm-derived palmitic acid—an electricity-free LAMP heater is capable of maintaining a reaction within the amplification window of 5°C to 45°C and maintains detection limits near those of a laboratory heat block. The model pinpoints the levers of significance such as type of phase change material, type of conductive filler and water metering and climate-matched fuel dosing, while also identifying pitfalls like raw beeswax or over-insulation. It provides a cost-effective way to carry out molecular tuberculosis and malaria testing at sites lacking dependable electricity, and a free option to tailor the design for other isothermal tests..

Abbreviations

CaO
calcium oxide (quicklime)
DSC
differential scanning calorimetry
LAMP
loop-mediated isothermal amplification
LoD95
limit of detection at 95% probability
Mg–Fe
magnesium–iron alloy
NINA
non-instrumented nucleic acid amplification
PCM
phase-change material
TB
tuberculosis

Declarations

Ethics approval and consent to participate

Not applicable. This study used computer simulation only.

Consent for publication

Not applicable.

Availability of data and materials

All simulation code, input parameters and scripts that regenerate the figures and Tables are included as Additional file 1 and will be uploaded to a public repository (Zenodo) upon acceptance.

Competing interests

The authors declare that they have no competing interests.

Funding

Not Applicable

Authors' contributions

OAK: Conceptualization, methodology, investigation, project administration, and writing – original draft. OT: Methodology, data curation, simulation analysis, and visualization. AOB: Supervision, methodology, validation, formal analysis, and writing – review and editing. ASA: Software development, numerical modelling, simulation, and validation. DD: Biomedical application assessment, diagnostic methodology, and writing – review and editing. EED: Data analysis, visualization, and interpretation of simulation results. EOO: Technical review, validation planning, and writing – review and editing. All authors reviewed and approved the final manuscript and agreed to be accountable for their contributions.

Use of AI tools

The assistance of Claude (Anthropic), an AI system, under the direction of the authors was used to validate the simulation code. The authors take full responsibility for the content, in line with Springer Nature's policy on AI-assisted work.

Acknowledgements

The authors acknowledge the technical and administrative staff of the Department of Biomedical Engineering, Electrical and Information Engineering, Achievers University Owo, Nigeria, for assistance, equipment support and access to workshop facilities throughout the period of the simulation. The authors also acknowledge colleagues at the participating institutions for their feedback and support.

References

1. World Health Organization. Malaria fact sheet. Geneva: WHO; 4. December 2025. https://www.who.int/news-room/fact-sheets/detail/malaria

2. WHO Regional Office for Africa. African region records further decline in TB deaths and cases. Brazzaville: WHO AFRO; 2025. https://www.afro.who.int/news/african-region-records-further-decline-tb-deaths-cases.
3. World Health Organization. The use of loop-mediated isothermal amplification (TB-LAMP) for the diagnosis of pulmonary tuberculosis: policy guidance. Geneva: WHO; 2016. https://www.who.int/publications/i/item/9789241511186.
4. Notomi T, Okayama H, Masubuchi H, Yonekawa T, Watanabe K, Amino N, Hase T. Loop-mediated isothermal amplification of DNA. Nucleic Acids Res. 2000;28(12):e63.
5. Mori Y, Notomi T. Loop-mediated isothermal amplification (LAMP): a rapid, accurate, and cost-effective diagnostic method for infectious diseases. J Infect Chemother. 2009;15(2):62–9.
6. Goto M, Honda E, Ogura A, Nomoto A, Hanaki K. Colorimetric detection of loop-mediated isothermal amplification reaction by using hydroxy naphthol blue. Biotechniques. 2009;46(3):167–72.
7. World Health Organization. Electricity in health-care facilities. Fact sheet. Geneva: WHO. 2026. https://www.who.int/news-room/fact-sheets/detail/electricity-in-health-care-facilities. See also WHO, World Bank, SEforALL, IRENA. Energizing health: accelerating electricity access in health-care facilities. Geneva: WHO; 2023.
8. LaBarre P, Hawkins KR, Gerlach J, Wilmoth J, Beddoe A, Singleton J, Boyle D, Weigl B. A simple, inexpensive device for nucleic acid amplification without electricity—toward instrument-free molecular diagnostics in low-resource settings. PLoS ONE. 2011;6(5):e19738. [verify page/article number].
9. LaBarre P, Gerlach J, Wilmoth J, Beddoe A, Singleton J, Weigl B. Non-instrumented nucleic acid amplification (NINA): instrument-free molecular malaria diagnostics for low-resource settings. Conf Proc IEEE Eng Med Biol Soc. 2010;2010:1097–9. [verify].
10. Liu C, Mauk MG, Hart R, Qiu X, Bau HH. A self-heating cartridge for molecular diagnostics. Lab Chip. 2011;11(16):2686–92. 10.1039/c1lc20345b.
11. Curtis KA, Rudolph DL, Nejad I, Singleton J, Beddoe A, Weigl B, LaBarre P, Owen SM. Isothermal amplification using a chemical heating device for point-of-care detection of HIV-1. PLoS ONE. 2012;7(2):e31432. 10.1371/journal.pone.0031432.
12. Singleton J, Osborn JL, Lillis L, Hawkins K, Guelig D, Price W, et al. Electricity-free amplification and detection for molecular point-of-care diagnosis of HIV-1. PLoS ONE. 2014;9(11):e113693. [verify article number].
13. Shah KG, Guelig D, Diesburg S, Buser J, Burton R, LaBarre P, Richards-Kortum R, Weigl B. Design of a new type of compact chemical heater for isothermal nucleic acid amplification. PLoS ONE. 2015;10(10):e0139449. 10.1371/journal.pone.0139449.
14. Adoghe OB, Noor GM. Overcoming efficiency barriers in the optimization of heat exchangers for enhanced energy recovery in industrial systems. Pak Adv Eng Res. 2024;1(2):43–53.
15. IndexBox. Africa – beeswax – market analysis, forecast, size, trends and insights. 2025. https://www.indexbox.io/blog/beeswax-africa-market-overview-2024-5/

16. Voller VR, Prakash C. A fixed grid numerical modelling methodology for convection–diffusion mushy region phase-change problems. Int J Heat Mass Transf. 1987;30(8):1709–19.
17. Gustafsson T, McBain GD. scikit-fem: a Python package for finite element assembly. J Open Source Softw. 2020;5(52):2369.
18. Haynes WM, editor. Standard enthalpies of formation of CaO, $Ca(OH)_2$, $Mg(OH)_2$ and H_2O. CRC Handbook of Chemistry and Physics. 97th ed. Boca Raton: CRC; 2016.
19. Flameless heater and method of making same. US Patent 5,611,329. (Composition and hydrogen release of Mg–Fe ration heaters.).
20. Jander W. Reaktionen im festen Zustande bei höheren Temperaturen. Z Anorg Allg Chem. 1927;163(1):1–30.
21. Mishra AK, Lahiri BB, Solomon V, Philip J. Nano-inclusion aided thermal conductivity enhancement in palmitic acid/di-methyl formamide phase change material for latent heat thermal energy storage. Thermochim Acta. 2019;678:178309. 10.1016/j.tca.2019.178309.
22. Sharma A, Tyagi VV, Chen CR, Buddhi D. Review on thermal energy storage with phase change materials and applications. Renew Sustain Energy Rev. 2009;13(2):318–45.
23. Schuman Y. Thermal analysis of phase change materials – three organic waxes using TGA, DSC, and modulated DSC. Application note TA405. New Castle, DE: TA Instruments.
24. Carslaw HS, Jaeger JC. Conduction of Heat in Solids. 2nd ed. Oxford: Clarendon; 1959.
25. Sobol IM. Global sensitivity indices for nonlinear mathematical models and their Monte Carlo estimates. Math Comput Simul. 2001;55(1–3):271–80.
26. Saltelli A, Annoni P, Azzini I, Campolongo F, Ratto M, Tarantola S. Variance based sensitivity analysis of model output. Design and estimator for the total sensitivity index. Comput Phys Commun. 2010;181(2):259–70.
27. Herman J, Usher W. SALib: an open-source Python library for sensitivity analysis. J Open Source Softw. 2017;2(9):97.
28. Adoghe OB, Raza W. Computational approaches to enhancing the thermal management of wiring systems in high-power electronics. J Eng Educ Pract. 2024;2(2):27–36.

Figures

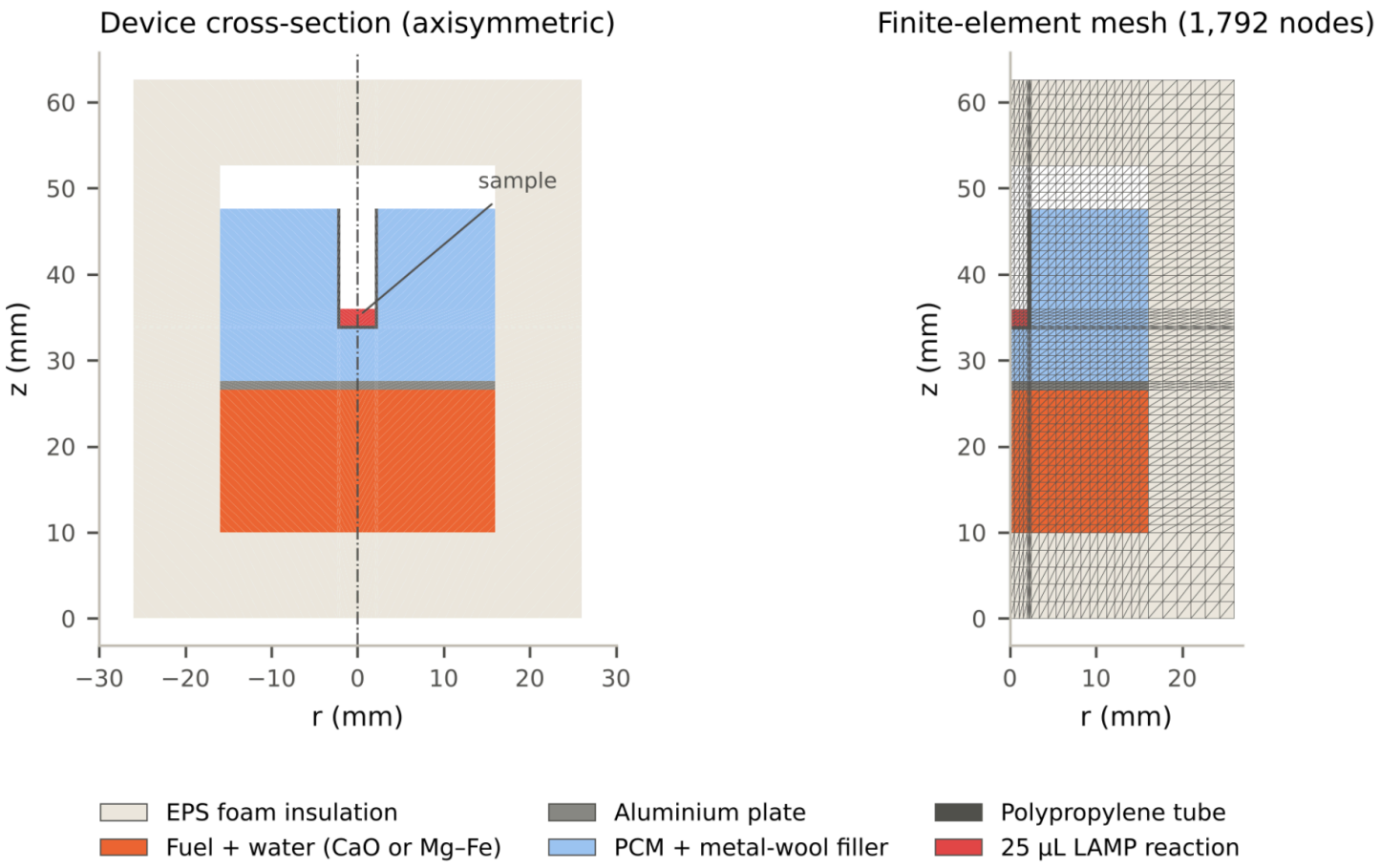

Figure 1

Modelled heater. (a) Axisymmetric cross-section: foam cup, fuel and water bed, aluminium plate, PCM with metal-wool filler, and a 0.2 mL tube holding 25 µL of LAMP mix. Water is delivered to the fuel by a wick. (b) Finite-element mesh aligned with all material interfaces (reference resolution shown).

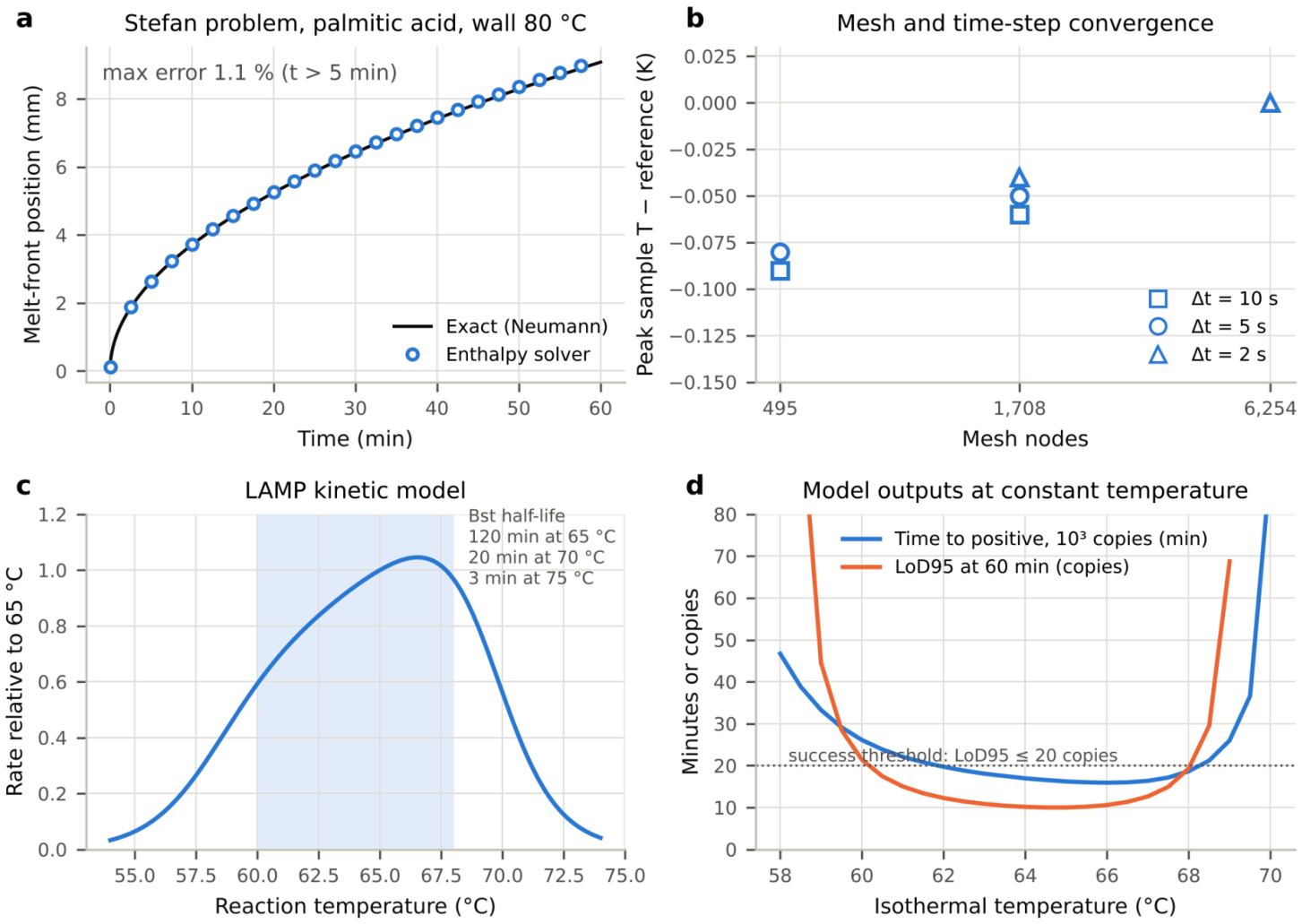

Figure 2

Verification and LAMP model. (a) Melt-front position for planar melting of palmitic acid: enthalpy solver against the exact Neumann solution. (b) Change in peak sample temperature with mesh size and time step relative to the finest run. (c) Relative LAMP amplification rate against temperature, with the 60–68 °C window shaded. (d) Isothermal time-to-positive (10³ copies) and LoD95 at a 60-minute read; the dotted line marks the validity threshold of 20 copies.

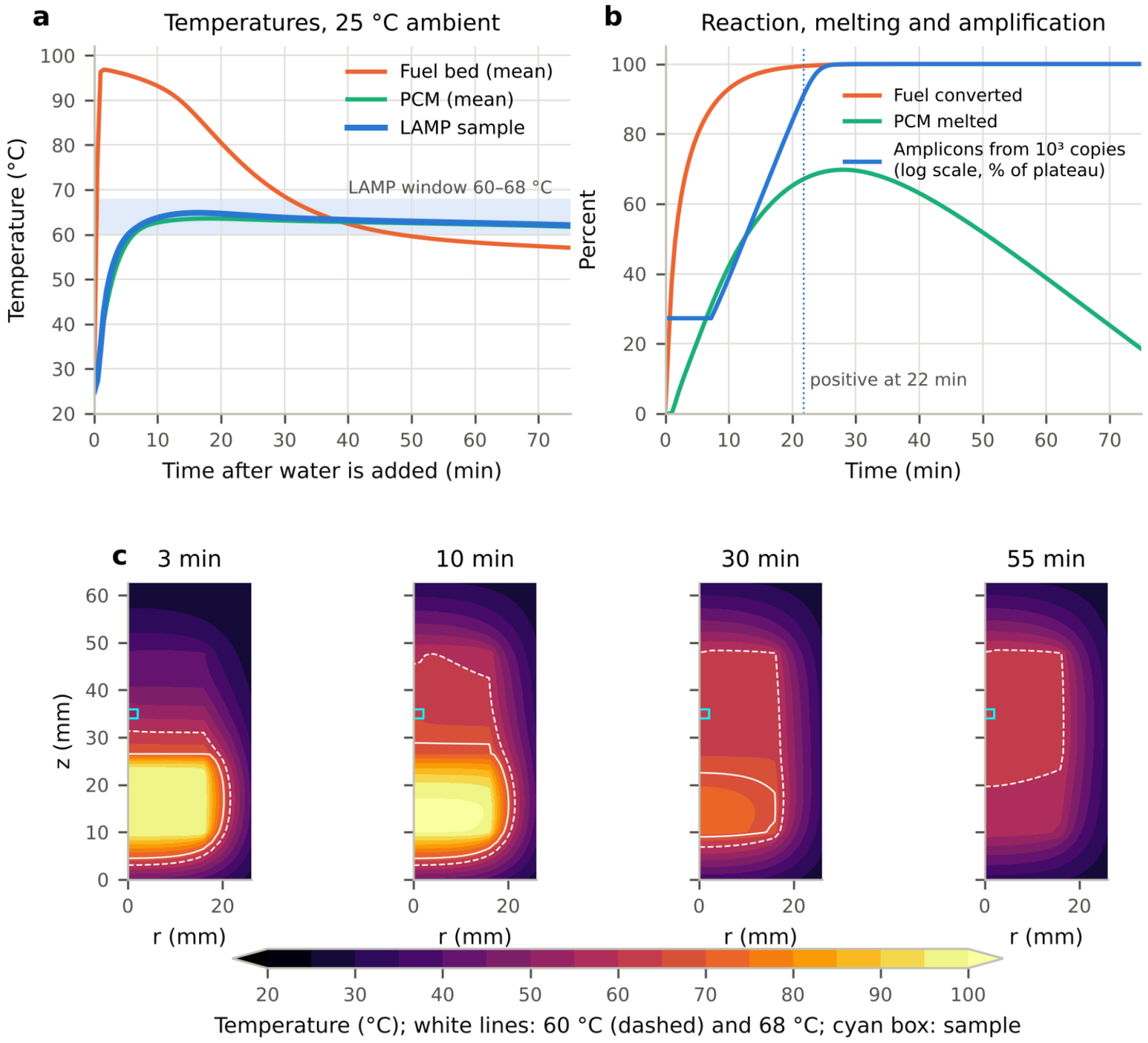

Figure 3

Optimised quicklime heater at 25 °C ambient (12 g CaO, palmitic acid, 8× filler). (a) Mean fuel-bed, PCM and sample temperatures. (b) Fuel conversion, PCM molten fraction and amplicon growth from 10³ copies (log scale). (c) Temperature fields at 3, 10, 30 and 55 min; white lines mark 60 °C (dashed) and 68 °C, and the cyan box marks the sample.

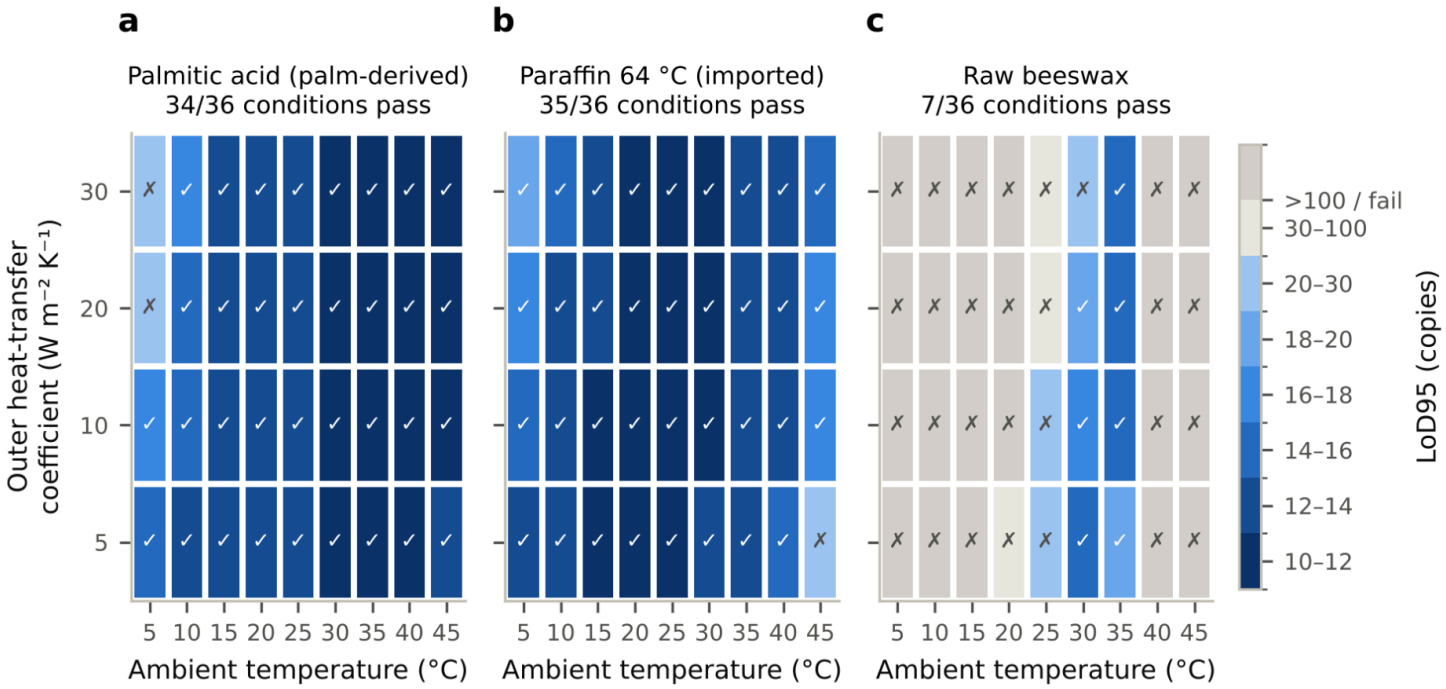

Figure 5

Climate maps for the optimised quicklime design. LoD95 at 60 min across ambient temperature and outer heat-transfer coefficient (still air to wind) for (a) palmitic acid, (b) paraffin and (c) raw beeswax. ✓ marks valid conditions (LoD95 ≤ 20 copies).

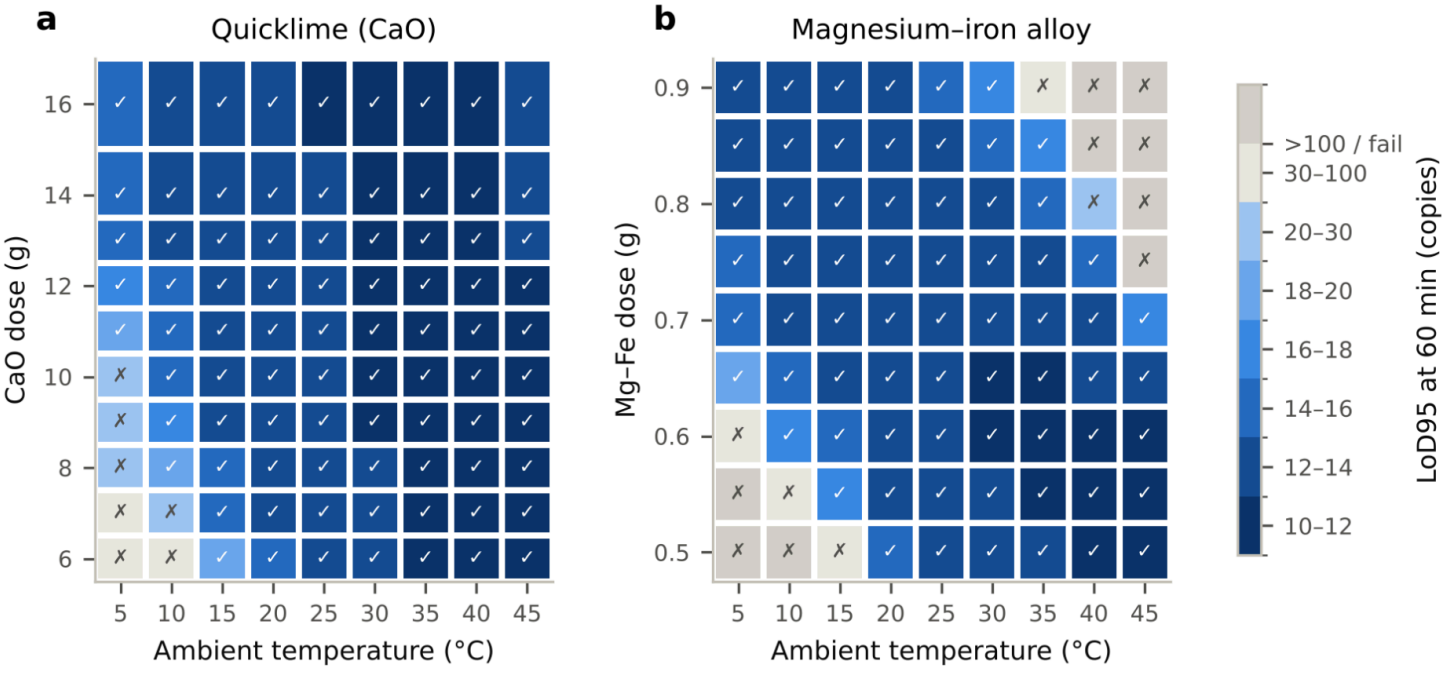

Figure 6

Dose windows. LoD95 against fuel dose and ambient temperature for (a) quicklime and (b) Mg–Fe alloy, both with palmitic acid. Quicklime is valid over a dose range about five times wider than Mg–Fe.

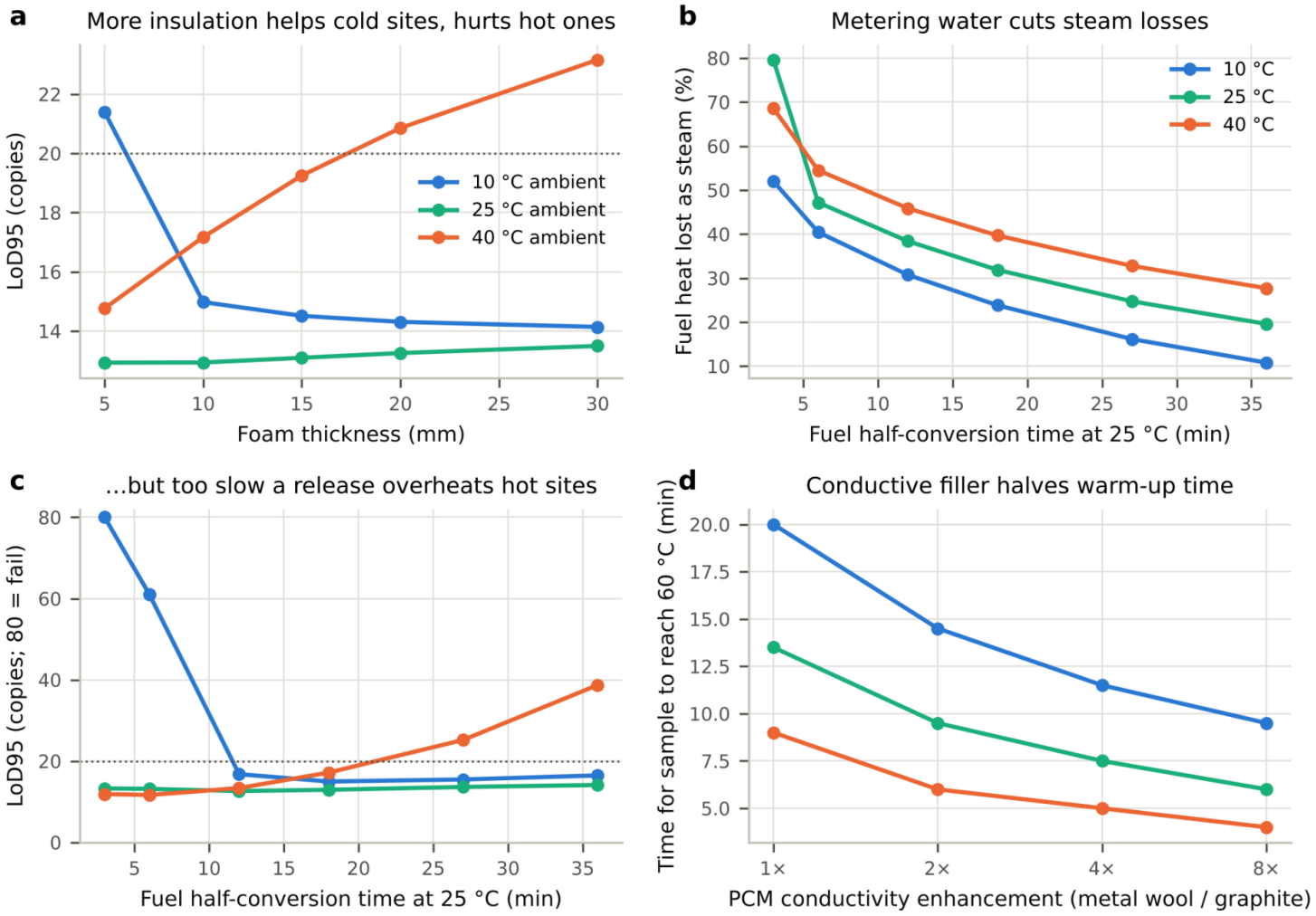

Figure 7

Design trade-offs (reference design). (a) Foam thickness improves cold-site but worsens hot-site LoD95. (b) Slower fuel release reduces heat lost as steam, (c) but too slow a release overheats hot sites. (d) Conductive filler in the PCM shortens warm-up.

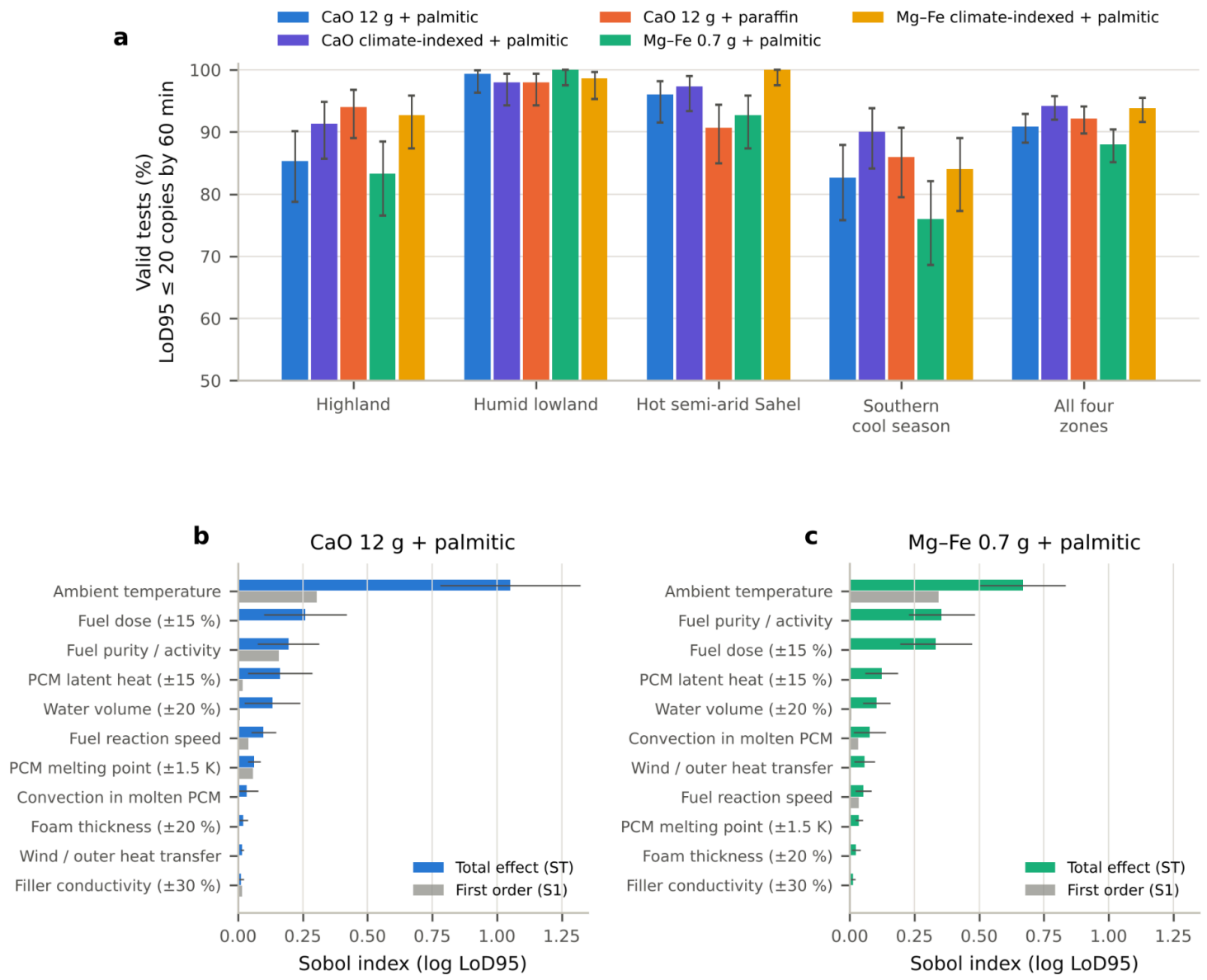

Figure 8

Reliability and sensitivity. (a) Percentage of valid tests in 150 Monte Carlo tests per climate zone and design, with Wilson 95% confidence intervals. Zones: highland (e.g. Addis Ababa, Nairobi; 8–24 °C), humid lowland (e.g. Lagos, Kinshasa; 23–33 °C), hot semi-arid Sahel (e.g. Kano, Niamey; 25–45 °C), southern cool season (e.g. Johannesburg, Lusaka; 3–22 °C). (b, c) Sobol first-order (S1) and total-effect (ST) indices of log LoD95 for the fixed quicklime and Mg–Fe designs over the full regional range (3–45 °C).

Supplementary Files

This is a list of supplementary files associated with this preprint. Click to download.

- Additionalfile1simulationcode.zip